ELSEVIER
Chemical Physics 281 (2002) 61–70
Chemical Physics
www.elsevier.com/locate/chemphys

The J-band of organic dyes: lineshape and coherence length ☆

Alexander Eisfeld, John S. Briggs *

Theoretische Quantendynamik, Fakultät für Physik, Universität Freiburg, Hermann-Herder-Strasse 3, D-79104 Freiburg, Germany

Received 26 February 2002

Abstract

Self-organised J-aggregates of dye molecules, known for over 60 years, are emerging as remarkably versatile quantum systems with applications in photography, opto-electronics, solar cells, photobiology and as supra-molecular fibres. Recently there has been much effort to achieve quantum entanglement and coherence on the nanoscale in atom traps and quantum dot aggregates (for use in quantum computing). We point out that the excitonic state of the J-aggregate is a text-book case of mesoscopic quantum coherence and entanglement. The establishment of coherence can *literally be seen* since the dye changes colour dramatically on aggregation due to strong shifts in the absorption spectrum. Here we reproduce in a simple theory the shifts and shapes of optical absorption spectra upon aggregation to a polymer and calculate the coherence length of quantum entanglement of monomer wavefunctions. © 2002 Published by Elsevier Science B.V.

1. Introduction

The polymeric exciton, a delocalised electronic excitation of an aggregate of N monomers, is arguably the paradigm of quantum entanglement on the nanoscale. In loose aggregates, the monomer molecules largely retain their character and the exciton state is described by a coherent linear superposition of states in which only one monomer on the chain carries the electronic excitation. With the simplifying assumption of circular boundary conditions the entangled states k of the exciton band are

$$|\Psi_k\rangle = \frac{1}{\sqrt{N}} \sum_n \exp(\mathrm{i}kn)|\pi_n\rangle, \qquad (1)$$

where $|\pi_n\rangle$ is a product of monomer states in which the nth monomer is excited electronically and all others are in their ground state. In nearest-neighbour approximation the exciton energies are given simply by

$$E_k = E_0 + 2J\cos(k), \qquad (2)$$

where E_0 is the monomer transition energy and J is the transition dipole–dipole interaction between nearest neighbours. Under the influence of this interaction, excitation propagates coherently along the polymer chain and in the absence of dissipation the coherence and propagation length is as large as the polymer. According to (1) and (2) each coherent exciton state of given k has a different energy so that in the polymer the single monomer

---

☆ This paper is dedicated to Arvid Herzenberg, Professor Emeritus, Yale University.

* Corresponding author. Fax: +761-203-5755.

E-mail address: briggs@physik.uni-freiburg.de (J.S. Briggs).

0301-0104/02/$ - see front matter © 2002 Published by Elsevier Science B.V.
PII: S0301-0104(02)00594-3

excited state splits into a band of N excitonic states.

A striking manifestation of the formation of such an entangled mesoscopic state is the *J*-band [1,2] of a class of photosensitising dyes, typified by pseudoisocyanine chloride (PIC) and the dye TDBC. These dye molecules aggregate simply when concentrated in solution. The aggregation is accompanied by a dramatic change in the spectrum, see Fig. 1. In the case of TDBC the monomer shows a broad absorption band with vibrational structure. The polymer spectrum is a single band, called the *J*-band, strongly shifted to lower energies and *extremely narrow*, showing no vibrational structure at all. Simple exciton theory [3] shows that the coherence of the excitation, described by Eq. (1), implies that only the exciton state where all transition dipoles are in phase absorbs light. The reason for the extreme narrowness of the *J*-band is more subtle and is one of the subjects of this paper.

Although observed and recognised for over 60 years [1–5], the *J*-band formation in dye molecules has been the subject of a strong resurgence of interest lately. Apart from fundamental scientific interest, such as the demonstration of superradiance [6,7] and that optical activity due to spontaneous chiral symmetry breaking is generated on aggregation [8], there are numerous technical applications being explored. For example, PIC forms self-assembled supramolecular flexible fluorescent fibres [9] which have important applications in thin-film optical and optoelectronic devices. The use as optically bistable devices, as photoconductors, optical logical elements, in the construction of electroluminescent devices and in Graetzel solar cells have all been suggested [10]. These dyes can be used to form organic semiconductor microcavities [11]. They have long been used as sensitising agents in colour photography. Cyanine dyes bind to DNA as template [12] and exciton formation is believed to be important in photobiology, for example in the light-harvesting photosynthetic unit [13]. The colour changes of β-carotene are due to the degree of aggregation into supramolecular structures of the *J*-aggregate [14].

Clearly, the coherent propagation of electronic excitation will be affected by coupling to vibrations and correspondingly this will show up in the aggregate spectrum. This decoherence will also decide the precise exciton propagation length i.e. the curtailing of the infinite propagation predicted by the vibrationless exciton theory. Several theories describing principally the effect of lattice vibrations have been developed [15–18], mostly using a model second quantised Hamiltonian. A Green function approach incorporating both intra- and intermolecular vibrations was put forward long ago [19,20]

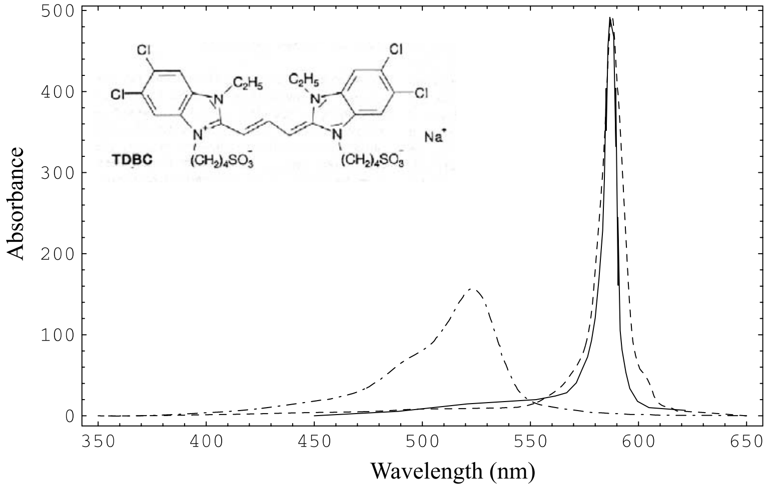

Fig. 1. The absorption spectrum of the dye TDBC. The absorbance is in arbitrary units. Dot-dash line: the monomer spectrum. Continuous line: the *J*-aggregate spectrum. Dashed line: the theoretical *J*-aggregate spectrum, with $C = -2416\ \mathrm{cm}^{-1}$.

but, due to lack of experimental data was not applied in detail. This approach, called the “coherent exciton scattering” (CES) theory, relates in a rather simple way the precise *shape* of the polymer spectrum to the monomer spectrum. The average energy (first moment) of the polymer spectrum is shifted from that of the monomer by exactly the interaction energy between monomers [21]. The revived interest in *J*-aggregate spectra, the availability of new measurements and particularly the topicality of entanglement and coherence on a mesoscopic scale prompts us to apply the CES approximation to calculate the detailed bandshape of polymer absorption for a variety of dye aggregates. We show that this extremely simple theory gives very close agreement with measured *J*-aggregate spectra. More importantly, it allows an estimate to be made of the length of coherent propagation of an exciton in the *J*-band before coupling to vibrations interrupts this process.

Experiments in the 1930s showed that the dye molecule 1,1′-diethyl-2,2′-cyanine chloride (PIC), aggregates spontaneously in solution into rod-like structures, and that such aggregation is accompanied by *J*-band formation. This narrow, shifted polymer absorption band was first observed by Jelley [1] and by Scheibe [2] in 1936. It was recognised by Franck and Teller [22] in 1938 that the electronic state, called a “communal state” by Scheibe, is a cooperative electronic excitation of the polymer as a whole. They also identified it as an ‘excitation wave’ or exciton as proposed by Frenkel [23] for molecular crystals. Frenkel saw the close analogy of the exciton to a coherent de Broglie matter wave. Discovered by chemists, the *J*-aggregate exciton is perhaps the first demonstration in physics of a delocalised entangled quantum state on a nano or even mesoscopic scale. Although exciton theories in which electron excitation alone is considered suggest correctly the position of the polymer band peak, they give no clue as the *shape* of absorption bands in the polymer. The CES theory provides the polymer exciton absorption bandshape and using this theory it was shown explicitly [19] that the extreme narrowness of the *J*-band compared to the monomer band is due to the rapid transfer of the electronic excitation along the polymer, before an individual excited monomer has time to form a well-defined vibrational eigenstate and before vibrational relaxation to modes external to a single chromophore can occur.

The renewed interest in the absorption spectra of such dye molecules, has been fuelled by the above-mentioned technical applications. Crucial for these applications is a knowledge of the precise geometrical structure of the self-organised dye aggregate, since function may be optimised if this structure can be influenced. The exciton formation is due to dipole–dipole coupling of the monomer transition dipoles and hence elementary exciton theory predicts a strong dependence of the absorption band on the precise geometry of the aggregate. For example, for PIC linear, two-dimensional “brick-wall” and helical structures have all been suggested. Indeed by comparing theoretical predictions with the observed spectra it is possible to obtain evidence as to the structure of the aggregate. In the following, detailed quantitative comparison of measured polymer dye spectra with the predictions of the CES approximation are made. In particular an explicit estimate of the coherence length of exciton propagation is given and the strong dependence of this length on the coupling strength between monomers is demonstrated.

2. The CES approximation

The CES approximation is a one-band exciton model in which the various exciton–phonon couplings, in particular the intramolecular vibrations which largely determine the monomer bandshape, are included implicitly by relating the polymer absorption bandshape directly to that of the monomer. The precise relationship depends upon the aggregate geometry. Although, within the one-band approximation, the theory gives the absolute magnitude of the absorption cross-section, interest is centred here on the *shape* of the polymer absorption band w.r.t. that of the monomer. As shown in Appendix A, for a variety of aggregate geometries, including linear stack and helical, this relationship is expressed through bandshape functions, $\langle G(E)\rangle$ for polymer and $\langle g(E)\rangle$ for monomer as [19],

$$\langle G(E)\rangle = \langle g(E)\rangle[1 - C\langle g(E)\rangle]^{-1}. \tag{3}$$

Here E is the energy position in the corresponding absorption band whose shape is given by $-\mathrm{Im}\langle G(E)\rangle$ for polymer and $-\mathrm{Im}\langle g(E)\rangle$ for monomer. The energy C is essentially the geometry-dependent dipole–dipole interaction energy of all monomers in the aggregate. In nearest-neighbour approximation $C = 2J$, as in Eq. (2). A one-band theorem [21] whose validity is preserved in the CES approximation, shows that C is precisely the difference between the first moment (mean absorption energy) of the polymer band and the first moment of the monomer band. The functions $\langle g\rangle$, $\langle G\rangle$ are complex functions but the real and imaginary parts are connected through the principal value integral by the dispersion relation

$$\mathrm{Re}f(E) = \frac{1}{\pi}P\int_{-\infty}^{\infty}\frac{\mathrm{Im}f(E')}{E' - E}\,\mathrm{d}E' \tag{4}$$

with $f = \langle g\rangle$ for monomer or $f = \langle G\rangle$ for polymer. The monomer absorbs at energies where $\mathrm{Im}\langle g(E)\rangle$ has poles (zeros in the denominator). The polymer absorbs where $\mathrm{Im}\langle G(E)\rangle$ has poles. Hence, from (3), the polymer absorbs at energies where $\mathrm{Re}\langle g(E)\rangle = 1/C$, since C is real. The main point we wish to emphasise is that the formula (3) allows the *shape* of the polymer band to be predicted solely from the monomer shape by taking $\mathrm{Im}\langle g(E)\rangle$ and C from experiment, calculating $\mathrm{Re}\langle g(E)\rangle$ from (4) and then the polymer spectrum from (3). The theory then has no free parameters. However, in many cases the monomer spectrum is not known precisely enough in the wings of the spectrum and it may be practically a better strategy to fit $\mathrm{Im}\langle g(E)\rangle$ to known functions and to treat C as a fit parameter. In any case, the polarisation of the absorption band and the sign and magnitude of the shift C depend upon the aggregate geometry, and hence the theory can be used to determine possible aggregate structures.

3. Dye aggregate spectra in the CES approximation

The first example we consider is the simplest, that of the dye TDBC. It is simplest in that the monomer spectrum shows only one broad peak with a shoulder on the high-energy side. The dye aggregates at relatively low concentrations apparently into a single structure showing only a clearly-defined narrow J-band and very low absorption in the monomer region [24], see Fig. 1. The simplicity of the polymer spectrum suggests an essentially linear structure so that Eq. (3) is directly applicable.

The first step is to calculate the real part of the monomer function according to Eq. (4) from the measured monomer absorption band. Unfortunately the monomer spectrum is only given in [24] down to 450 nm. Hence it is necessary to extrapolate to shorter wavelengths, although this has a negligible influence on the final result, since the shift is to longer wavelengths. The $\mathrm{Re}\langle g(E)\rangle$ obtained from the monomer spectrum is shown in Fig. 2. The single crossing of the energy axis by the dispersion curve is typical of the single peak nature of the monomer spectrum. If we write explicitly for the complex functions $\langle G\rangle = G_R + \mathrm{i}G_I$ and $\langle g\rangle = g_r + \mathrm{i}g_i$, a simple calculation shows that the polymer bandhape is given by

$$G_I = \frac{1}{C}\frac{Cg_i}{(1 - Cg_r)^2 + C^2g_i^2}. \tag{5}$$

This spectral energy function has a pole, giving strong absorption, when $g_r = 1/C$. From Fig. 1 one sees that the resulting polymer spectrum for $C = -2416\ \mathrm{cm}^{-1}$ is in excellent agreement in position *and shape* with the measured spectrum.

The simple structure of Eq. (3) allows the shape of the polymer band to be explained. From Fig. 2 one sees two poles when $g_r = 1/C$. The one at 575 nm gives rise to the J-band absorption. From Eq. (5) one sees that (Cg_i) acts as a 'width' to the band and since the polymer absorption, and hence g_i, is extremely small in this region, the width is small and the J-band narrow. This is a general feature; strong narrowing of the J-band is expected only when C is large enough to shift the pole to regions where the monomer does not absorb. Physically, C larger than the monomer bandwidth is the strong-coupling case where the exciton transfer time is much shorter than the vibrational relaxation time. The pole at 540 nm in the monomer absorption region, by contrast, has a large width Cg_i and this pole gives rise to a

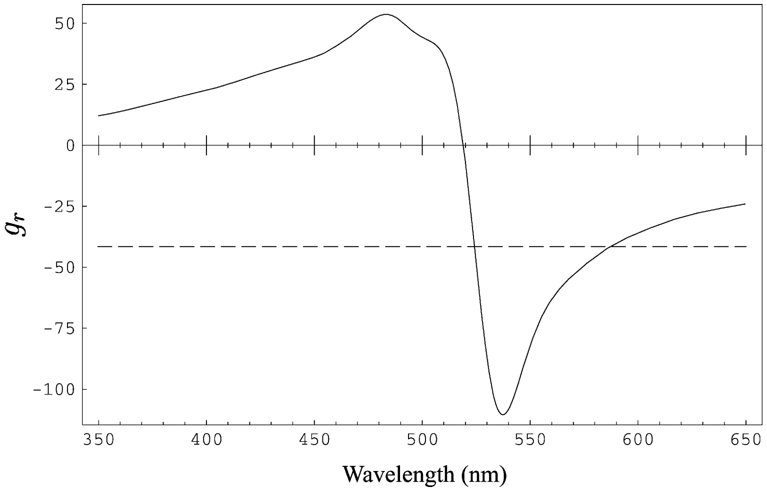

Fig. 2. The real part of the monomer function $\langle g(E)\rangle$ as a function of wavelength in nm. The horizontal line denotes the value of $1/C$ corresponding to $C = -2416$ cm^{-1}.

broad flat shoulder of absorption on the low wavelength side of the *J*-band.

We emphasise that once the monomer absorption, i.e., the spectral function $g_i(E)$, and the coupling strength C are fixed, the entire shape of the polymer spectrum is determined. Indeed in the favourable conditions applying to TDBC, the value of C can be extracted from the measured spectra as the difference in first moments of monomer and polymer spectra. The value of C used in Fig. 1 corresponds exactly to the shift of first moments, so that the comparison of theoretical and experimental polymer spectra has no external input other than the fit of the polymer peak height, which is necessary anyway as monomer and polymer spectra were not taken for a fixed number of monomers. This agreement can be taken as confirmation of the validity of the assumptions underlying the CES approximation.

The second example we consider is a modification of TDBC called TDBC/C8, differing from it by the substitution of carbon chains on one side of the molecule. These chains are hydrophobic. This derivative shows an identical monomer spectrum as TDBC itself. The polymer spectrum, however, is changed dramatically as shown in Fig. 3. Apart from the *J*-band at 605 nm there is an additional strong peak at 575 nm. This change has been attributed to a structural change in the aggregate. Due to the hydrophobic nature of the side chains, the polymer has a cylindrical, helical structure with the carbon chains on the inside of the cylinder. As has been shown in [19], a helical structure is expected to give rise to two bands of different polarisation with respect to the cylinder axis.

The theory shows that both polymer bandshapes are described by Eq. (1), the only difference being the value of the interaction C, which depends upon the orientation of the monomer transition dipole w.r.t. the helix axis. Using the measured monomer spectrum as input and two values of $C = C_\perp$, $C_\parallel$ as fit parameters, corresponding to polarisation perpendicular and parallel to the helix axis, the CES predictions for these two bands are shown in Fig. 3. Although the two bands are of different character, both shapes are well reproduced from Eq. (1). It should be emphasised that only a *single* scaling parameter has been used to fit the peak heights of *both* bands. This suggests that the bands do occur from a single aggregate type and not from two different aggregates.

The above finding is entirely in agreement with the conclusions of Spitz and Daehne [24] who observed that the two bands around 575 and 605 nm change intensity in the same way when solvent

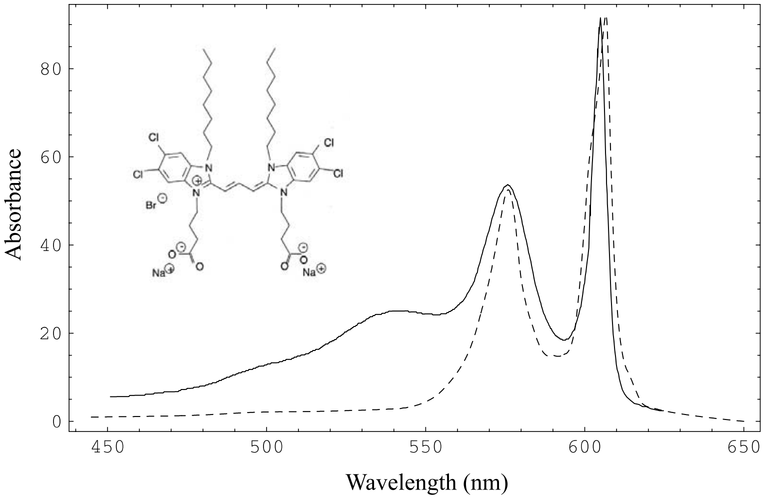

Fig. 3. The J-aggregate absorption spectrum of TDBC/C8. Continuous line; the measured spectrum. Dashed line: the theoretical spectrum. The J-band at 605 nm is polarised parallel, that at 575 nm perpendicular, to the helix axis. Interaction energies are $C_{\perp} = -2010\ \mathrm{cm}^{-1}$ and $C_{\|} = -2930\ \mathrm{cm}^{-1}$.

character and concentration changes. Their experiments also suggest that the band near 545 nm, not given by exciton theory, is to be attributed to absorption by residual monomers or dimers.

The last example is the classic case of PIC and here we use very recent measurements [25] to compare with theory. The monomer spectrum Fig. 4a shows a barely resolved vibrational progression. The J-aggregate shows the narrow J-band peak at 572 nm but also considerable absorption in the monomer region. The calculated J-band shape, using the measured monomer spectrum of g_i and a coupling strength of $-1940\ \mathrm{cm}^{-1}$, is in excellent agreement with experiment in the 572 nm region. However, the theory predicts negligible absorption in the monomer region. Remarkably, even after 60 years, the precise aggregation state of PIC is not settled. The results presented here suggest strongly that the absorption in the monomer region is not due to the J-aggregate. The precise admixture of monomer, dimer and H-aggregate spectra is not clear. However, although all experiments agree on the J-band, the absorption measured in the monomer region differs widely, indicating that this contribution is not from the J-aggregate. Indeed, very early experiments by Scheibe [26] on J-aggregates in streaming solution where the polymers are aligned, showed in parallel polarisation a pronounced J-band but very low absorption in the monomer region. This is in agreement with the calculation shown in Fig. 4.

4. Coherence of exciton propagation

The crucial variable in exciton propagation is the propagation distance, denoting the distance over which quantum coherence, i.e., the entangled state represented by Eq. (1), is preserved. In the purely electronic case, there is no decoherence and propagation over the complete polymer is established. In this case the k value in Eq. (1) is purely real. The coupling to vibrations and the decoherence have the consequence that k in Eq. (1) becomes complex. The propagation distance can be estimated, again using as input only the monomer spectrum and the coupling strength.

As shown in [19], the probability to pass from monomer m to monomer n is proportional to $|\langle G_{nm}(k)\rangle|^2$, where

$$\langle G_{nm}(k)\rangle = A_k \exp(\mathrm{i}k|n-m|) \tag{6}$$

with

$$A_k = \frac{\mathrm{i}}{C\sin k} \tag{7}$$

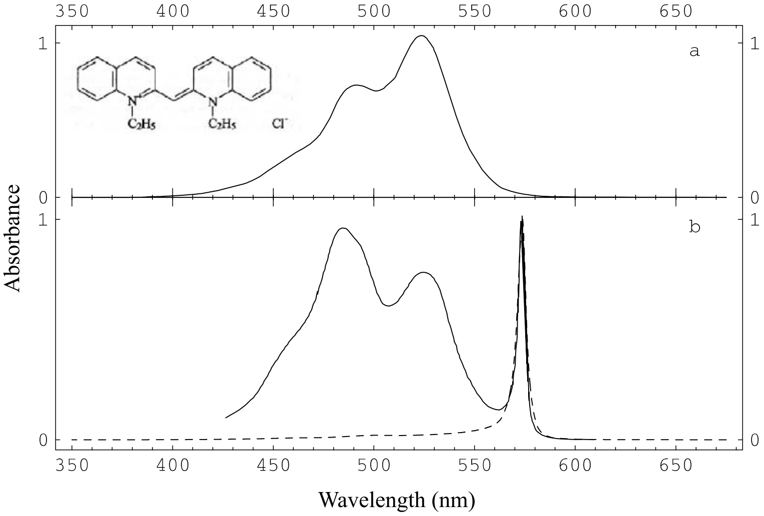

Fig. 4. (a) The monomer spectrum of the dye PIC; (b) continuous line; the measured aggregate spectrum. Dashed line: the theoretical *J*-aggregate spectrum.

and

$$k = \cos^{-1}\left(\frac{1}{C\langle g(E)\rangle}\right) \tag{8}$$

in nearest-neighbour approximation. Note that $k(E)$ is a function of the absorption energy due to the appearance of $\langle g(E)\rangle$ in Eq. (8).

We have evaluated $|\langle G_{n0}(k)\rangle|^2$ for the case of the PIC spectrum and the results are shown in Fig. 5(a) as a function of the absorption wavelength and the number of monomers n over which coherent propagation takes place. One sees that propagation occurs only in the wavelength region of *J*-band absorption and in this region delocalisation over tens of monomers is possible. The effect of vibrational damping on excitation transfer can also be viewed as a decoherence through damping of the entangled state representing the exciton. If one writes $k = k_r + \mathrm{i}k_i$ then

$$\langle G_{n0}\rangle = A_k \exp(\mathrm{i}k_r n)\exp(-k_i n) \tag{9}$$

and one sees directly that the vibrationally induced k_i damps out the phase coherence, expressed through the factor $\exp(\mathrm{i}k_r n)$, of the exciton.

The interaction strength C corresponds to a monomer transfer time of $\hbar/C$. Hence, the smaller is C the longer is the transfer time and the more time is available for vibrations to dissipate the coherence. For small C a shorter coherent propagation length is expected and this is shown in Fig. 5(b) where the PIC monomer $\langle g\rangle$ function has been used but with a fictitious value of C roughly half of that in Fig. 5(a), which corresponds to the physical situation. Now one sees that the propagation in the *J*-band region is rapidly damped and a coherence length of only a few monomers would be expected.

Here we have shown that the CES theory, requiring as input only the monomer spectrum and the strength C of the dipole–dipole interaction between monomers, can account well for the shape of aggregate spectra. The narrowing of the *J*-band and the concomitant establishment of an entangled excitonic state depends upon C being large enough to shift the polymer absorption to a spectral region where the monomer absorption is very low. The same simple theory allows an estimate to be made of the coherence length (number of monomers) over which propagation of electronic excitation takes place.

With respect to the coherence of exciton propagation, the interesting question arises as to the possibility of manipulating this coherence. Clearly as the dipole–dipole interaction between the monomers increases the length of coherence increases and the *J*-band becomes narrower indi-

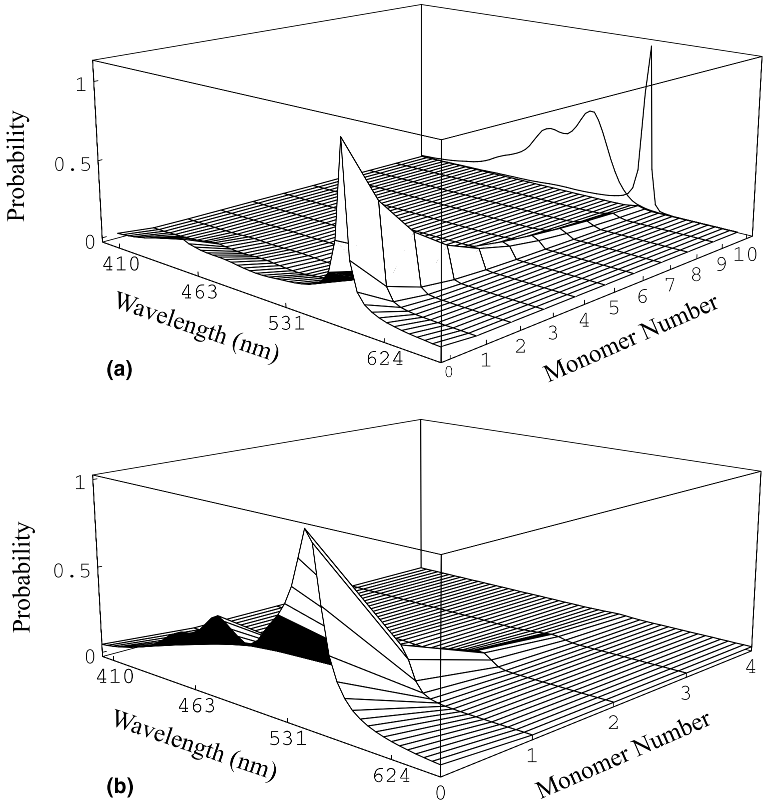

Fig. 5. The probability of coherent exciton propagation over n monomers in the J-aggregate of PIC as a function of wavelength: (a) with $C = -1940\ \mathrm{cm}^{-1}$ as obtained from experiment; (b) with a fictitious $C = -1000\ \mathrm{cm}^{-1}$. In (a) the absorption spectrum of monomer and J-aggregate are shown for comparison.

cating less and less coupling to vibrations. One way to achieve this is to apply pressure to the aggregate to squeeze the monomers together and such experiments have already been performed [24]. Another method would be to modify the aggregate spectrum by changing its geometry by chemistry, as in the modification of TDBC to TDBC/C8, or by binding to a DNA template [12]. Even more simple would be to lower the temperature drastically so that the monomer spectrum becomes a well-resolved vibrational progression. The suppression of coupling to vibrations external to the monomer will lead to a strong sharpening of the J-band and a corresponding increase in coherence length. From this point of view recent experiments on PIC J-aggregates in a solid matrix [27], rather than in solution, offer the possibility of low temperature measurements.

The question of using and manipulating quantum coherence is currently popular with a view to quantum information processing. Already atomic dimers acting through dipole–dipole forces have been proposed as a design for two-qubit gates [28,29]. The analogue here is the dye dimer in which the excited state is simply a pair of levels, i.e., $n = 2$ and $k = 0, \pi$ in Eq. (1) to give

$$|\Psi_{1,2}\rangle = \frac{1}{\sqrt{2}}(|\pi_2\rangle \pm |\pi_1\rangle)$$

exactly as in the case of a pair of Rydberg atoms. Of course, as with atoms the dimer would have to be cooled to very low temperatures to prevent the monomer–monomer oscillations destroying coherence. Again as with atoms, the major decoherence effect is radiative and non-radiative emission from the electronically excited dimer levels. In the case of dyes this is the fluorescence loss back to the ground state, which is of course difficult to control.

Whether such uses can be found for cyanine dye dimers and polymers is at the moment pure speculation. Certain is that the remarkable properties already established for this class of dye molecules assure for them a colourful future.

Appendix A

Here we briefly re-iterate the results of [19,21]. The Green operator $G(E)$ is given by

$$G(E) = \frac{1}{E - H + \mathrm{i}\delta}, \tag{A.1}$$

where H is the full Hamiltonian of the polymer, i.e., it is the sum of the electronic Hamiltionians of each monomer, the electronic interaction between monomers (assuming no overlap) and the Hamiltonian for the vibrational degrees of freedom. The corresponding Green operator for non-interacting monomers is given by

$$g(E) = \frac{1}{E - H_0 + \mathrm{i}\delta}, \tag{A.2}$$

where $H = H_0 + V$ and V is the monomer–monomer electronic interaction. Then one has the identity

$$G = g + gVG. \tag{A.3}$$

The polymer absorption bandshape is proportional to the imaginary part of the tensor dipole polarisability which is given by

$$\underline{\underline{\alpha}}^P = \sum_{n,m} \underline{\mu}_n \langle G_{nm} \rangle \underline{\mu}_m, \tag{A.4}$$

where $\underline{\mu}_n$ is the transition dipole on monomer n and $G_{nm} = \langle \pi_n | G | \pi_m \rangle$. The vector $|\pi_m\rangle$ denotes a polymer state in which monomer m is excited electronically. The average $\langle \cdots \rangle$ denotes an integration over the vibrational ground state. After these integrations the operator equation (A.3) becomes

$$\langle G_{nm} \rangle = \langle g_n \rangle \delta_{nm} + \left\langle g_n \sum_{n'} V_{nn'} G_{n'm} \right\rangle. \tag{A.5}$$

The key approximation, the CES approximation, involves replacing the operator g_n in (A.5) by its vibrational average $\langle g_n \rangle$. With this simplification, it is shown in [19] that the diagonal component of the polarisability parallel to the axis of a helix composed of N monomers is

$$\alpha_{\parallel}^P = N \left(\frac{\langle g \rangle}{1 - C_{\parallel} \langle g \rangle} \right) \mu_z^2 \tag{A.6}$$

and perpendicular to it by

$$\alpha_{\perp}^P = N \left(\frac{\langle g \rangle}{1 - C_{\perp} \langle g \rangle} \right) \left(\mu_x^2 + \mu_y^2 \right). \tag{A.7}$$

Here

$$C_{\parallel} = \sum_n V_{nm} \tag{A.8}$$

with $V_{nm} = \langle \pi_n | V | \pi_m \rangle$. Similarly

$$C_{\perp} = \sum_n V_{nm} \mathrm{e}^{\mathrm{i}(n-m)\phi}, \tag{A.9}$$

where the helix rotation angle per monomer is ϕ. Note that the subscript n on $\langle g_n \rangle$ may be dropped since all monomers are identical.

The polymer absorption bandshape is given by the function

$$-\mathrm{Im} \langle G(E) \rangle \equiv -\mathrm{Im} \frac{\langle g(E) \rangle}{1 - C \langle g(E) \rangle} \tag{A.10}$$

with $C = C_{\parallel}$ or $C_{\perp}$. The monomer absorption bandshape function is simply $-\mathrm{Im}\langle g \rangle$. Note that $C_{\perp} = C_{\parallel}$ for $\phi = 0$ (linear stack).

References

[1] E.E. Jelley, Nature 138 (1936) 1009.
[2] G. Scheibe, Angew. Chem. 49 (1936) 563.
[3] A.S. Davydov, Theory of Molecular Excitons, McGraw-Hill, New York, 1962.
[4] W. Hoppe, Koll. Zeit. 109 (1944) 21.
[5] H. Zimmermann, G. Scheibe, Zeit. f. Elektrochemie 60 (1956) 566.
[6] F.C. Spano, J.R. Kuklinski, S. Mukamel, Phys. Rev. Lett. 65 (1990) 211.
[7] H. Fidder, J. Knoester, D.A. Wiersma, Chem. Phys. Lett. 171 (1990) 529.
[8] C. Spitz, S. Dähne, A. Ouart, H. Abraham, J. Phys. Chem. B 104 (2000) 8664.
[9] D.A. Higgins, J. Kerimo, D.A. Vanden Bout, P.F. Barbara, J. Am. Chem. Soc. 118 (1996) 4049.

[10] J. Moll, S. Dähne, J.R. Durrant, D.A. Wiersma, J. Chem. Phys. 102 (1995) 6362.
[11] P. Schouwink, H.V. Berlepsch, L. Dähne, R.F. Mahrt, Chem. Phys. Lett. 344 (2001) 352.
[12] J.O. Smith, D.A. Olson, B.A. Armitage, J. Am. Chem. Soc. 121 (1999) 2686;
A. Chowdhury, S. Wachsmann-Hogiu, P.R. Bangal, I. Raheem, L.A. Peteanu, J. Phys. Chem. B 105 (2001) 12196.
[13] S. Tretiak, C. Middleton, V. Chernyak, S. Mukamel, J. Phys. Chem. B 104 (2000) 4519.
[14] D. Horn, J. Rieger, Angew. Chem. Int. Ed. 40 (2001) 4330.
[15] H. Haken, G. Strobl, Z. Phys. 262 (1973) 135.
[16] H. Sumi, J. Chem. Phys. 67 (1977) 2943.
[17] E.W. Knapp, Chem. Phys. 85 (1984) 73.
[18] P.O.J. Scherer, S.F. Fischer, Chem. Phys. 86 (1984) 269.
[19] J.S. Briggs, A. Herzenberg, Mol. Phys. 21 (1971) 865.
[20] J.S. Briggs, Zeit. f. Phys. Chemie NF 75 (1971) 214.
[21] J.S. Briggs, A. Herzenberg, J. Phys. B 3 (1970) 1663.
[22] J. Franck, E. Teller, J. Chem. Phys. 6 (1938) 861.
[23] J. Frenkel, Phys. Rev. 37 (1931) 1276.
[24] C. Spitz, S. Daehne, Ber. Bunsen. Phys. Chem. 102 (1998) 738.
[25] B. Neumann, J. Chem. Phys. B 105 (2001) 8268.
[26] G. Scheibe, Palette No. 35 Sandoz AG, Basel, 1970.
[27] L.M. Ilharco, R. Brito de Barros, Langmuir 16 (2000) 9331.
[28] D. Jaksh, J.I. Cirac, P. Zoller, S.L. Rolston, R. Côté, M.D. Lukin, Phys. Rev. Lett. 85 (2000) 2208.
[29] G.K. Brennen, I.H. Deutsch, P.S. Jessen, Phys. Rev. A 61 (2000) 062309.